Characterization of boundary roughness of two cube grains in partly recrystallized copper

Sun, Jun; Zhang, Yubin; Dahl, Anders Bjorholm; Conradsen, Knut; Juul Jensen, Dorte

Published in:
I O P Conference Series: Materials Science and Engineering

Link to article, DOI:
10.1088/1757-899X/89/1/012044

Publication date:
2015

Document Version
Publisher's PDF, also known as Version of record

Characterization of boundary roughness of two cube grains in partly recrystallized copper

2015 IOP Conf. Ser.: Mater. Sci. Eng. 89 012044

(http://iopscience.iop.org/1757-899X/89/1/012044)

IOP Conf. Series: Materials Science and Engineering **89** (2015) 012044 doi:10.1088/1757-899X/89/1/012044

Characterization of boundary roughness of two cube grains in partly recrystallized copper

J Sun[1], Y B Zhang[1], A B Dahl[2], K Conradsen[2] and D Juul Jensen[1]
[1] Danish-Chinese Center for Nanometals, Section for Materials Science and Advanced Characterization, Department of Wind Energy, Technical University of Denmark, Risø Campus, 4000 Roskilde, Denmark
[2] Section for Image Analysis and Computer Graphics, Department of Applied Mathematics and Computer Science, Technical University of Denmark, Richard Petersens Plads, 2800, Kgs. Lyngby, Denmark

E-mail: jusu@dtu.dk

Abstract: Protrusions and retrusions typically form on recrystallizing boundaries and thus the boundaries often appear rough. Characterization of the boundary roughness is necessary in order to evaluate the effects of protrusions and retrusions on boundary migration. In the current work, a variable termed area integral invariant is employed to provide quantitative information of individual protrusions/retrusions on boundaries surrounding two selected recrystallizing grains in partly recrystallized copper as well as of the overall roughness of the boundaries.

1. Introduction

During the past few years, in-situ 3-dimensional X-ray diffraction (3DXRD) experiments have been used to observe the growth of recrystallizing grains in the bulk of deformed metals [1, 2]. It has been revealed that the nuclei do not grow in a homogeneous manner with constant moving speed as described in classic models, but occur with variations at the local scale: most boundary segment move in a jerky stop-go mode, with locally large protrusions and retrusions forming and disappearing as the boundary migrates [1, 2]. Ex-situ electron backscattered diffraction (EBSD) and electron channeling contrast (ECC) studies of local boundary migration have also revealed similar migration behavior [3-5]. Quantitative characterizations of local protrusions and retrusions have shown the importance of these local structural variations [4, 5]. Results from phase field simulations of boundary migration during recrystallization have shown that the protrusions and retrusions forming on the migrating boundaries may contribute an additional driving force resulting from the boundary curvature and change the migration kinetics at both the local and global scale [6]. Protrusions and retrusions have been observed in both high-purity metals and alloys, also under different thermal-mechanical processing conditions [7-9]. For analysis of the effects of protrusions/retrusions on the local boundary migration kinetic or for better knowledge of the effects of macro parameters such as purity of the metal, annealing temperature, deformation strain etc. on the formation of protrusions/retrusions, statistical quantification of protrusions/retrusions on many recrystallization boundaries in partly

recrystallized microstructures is required. One or more variables should be developed to describe the characteristics of individual protrusions/retrusions such as wavelength and amplitude as well as the overall roughness of many boundaries in a given sample.

2. Method to characterize boundary roughness

Efforts have been made in previous studies to provide a quantitative description of protrusions/retrusions. For example, Martorano et al. [10] have used a sinusoidal function to simulate boundary shape in a numerical analysis of growth during recrystallization. Zhang et al. [11] have applied both sinusoidal and polynomial functions to fit experimental data for protrusions/retrusions to calculate the local curvature driving forces. These methods are capable of quantitatively describing individual protrusions/retrusions. However, they are based on manual selections and are not suitable for statistical quantification of many protrusions/retrusions on a number of boundaries in a sample. Fractal analysis has been used in characterizing irregular and rough morphological features in the microstructure of materials [12, 13], since Mandelbrot made the correlation between the calculated fractal dimension of fracture surfaces and the impact energy for metals [14]. Whereas it is clear that neither fracture surfaces nor recrystallizing grain boundaries follow self-similarity which is the basis for obtaining fractal dimensions, analysis based on the fractal methods may be useful for characterization of recrystallizing boundaries as described in our previous work [15]. In the present work, a fully automatic method is presented and used to quantify the roughness of the boundaries surrounding two selected grains in a partly recrystallized copper sample. The same two grains were previously characterized using fractal analysis [15], however the new method presented here provides a significantly clearer description and is suitable for statistical quantification.

The area integral invariant (*AII*) is one of the integral invariants used in the digital image computing discipline for applications such as shape matching, geometry processing etc. [16,17]. In the current study, *AII* is modified to be a variable to quantify the boundary morphology. The method is schematically shown in figure 1: *AII* works by drawing a circle with a specified radius, termed *sampling radius*, and with the center of the circle placed on the boundary. Then the area of the circle is separated into two parts, the part within the recrystallized grain (marked as red in figure 1) and the other part within the deformed structure. The *AII* at a position is calculated with a specified sampling radius as:

$$AII = \frac{Circle\ area\ within\ recrystallized\ grain}{Area\ of\ the\ entire\ circle} \quad (1)$$

A number with a value between 0 and 1 is obtained: *AII* smaller than 0.5 indicates a protrusion at that position, and the smaller the value, the sharper is the protrusion; conversely for a retrusion; *AII* equals 0.5 for planar boundaries.

By measuring *AII* with a specified sampling radius along the boundary, a distribution of *AII* values for the whole boundary can be obtained and further statistical analysis can be done to characterize the roughness of the boundary. Several roughness parameters are further developed based on the distribution of *AII* to characterize various aspects of the boundary roughness (see table 1). The roughness of the boundary can be defined as the deviation of *AII* values from 0.5. As shown in table 1, the boundary roughness R_a is therefore calculated very similarly to the descriptive statistical parameter "coefficient of variation" but replacing the mean value with 0.5. $L_{boundary}$ is the total length of the boundary calculated by counting the pixels forming the boundary. Using a similar calculation process for only the *AII* data for protrusions or retrusions, the protrusion and retrusion roughness can be obtained as R_p and R_r, respectively. The L_p and L_r in the equation represent the length of boundary segments that are composed of pixels with $AII < 0.5$ (AII_p) and $AII > 0.5$ (AII_r), respectively. The *Range* is calculated as the difference between the maximum and minimum *AII* values. Finally the fraction of protrusions/retrusions is calculated as the total number of *AII* values that are

smaller than 0.4 or larger than 0.6 divided by the boundary length. This parameter provides an estimation of the fraction of rough features with respect to the entire boundary.

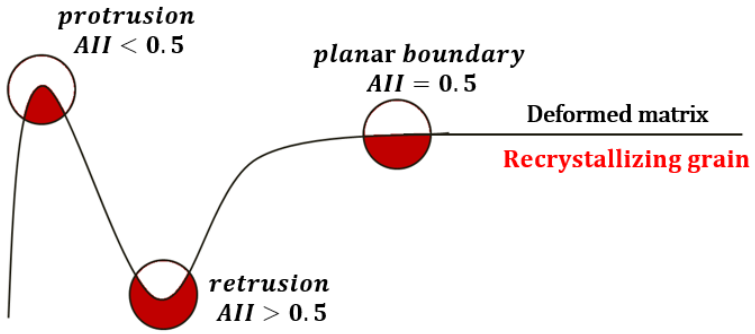

Figure 1. Sketch demonstrating the principle of how the *AII* is calculated. The deformed matrix is separated from the recrystallizing grain by the migrating boundary. The circle area is divided by the boundary into two regions and the *AII* is calculated as the area marked in red divided by the entire circle area.

Table 1. Roughness parameters

Roughness parameter	Calculation equation
Boundary roughness	$R_a = \left\{ \frac{\sum_{i=1}^{N} (AII_i - 0.5)^2}{L_{boundary}} \right\}^{\frac{1}{2}} / 0.5$
Fraction of protrusions/retrusions	$R_f = \frac{Number\ (AII < 0.4\ or\ AII > 0.6)}{L_{boundary}}$
Protrusion roughness	$R_p = \left\{ \frac{\sum_{i=1}^{Np} (AIIp_i - 0.5)^2}{L_p} \right\}^{\frac{1}{2}} / 0.5$
Retrusion roughness	$R_r = \left\{ \frac{\sum_{i=1}^{Nr} (AIIr_i - 0.5)^2}{L_r} \right\}^{\frac{1}{2}} / 0.5$
Range	$Range = AII_{max} - AII_{min}$

3. Experimental materials and boundary measurement

Two cube oriented grains in partly recrystallized microstructures are investigated. Both grains are from oxygen free high conductivity (OFHC) copper (99.9% purity) cold rolled to 90% reduction and annealed for 60 minutes at 150 °C. The EBSD images for both grains are shown in figure 2 as well as the boundaries of the grains after image processing with the interior twin boundaries removed. The two grains are designated as CuSC1 and CuSC2.

Visual inspection indicates that both CuSC1 and CuSC2 have rough boundaries, with protrusions and retrusions of various sizes formed on the boundaries. However, CuSC1 appears more irregular than CuSC2 as CuSC1 has some narrow branch-like features, whilst CuSC2 can be simply described as an elongated grain with some smaller protrusions/retrusions on the boundary.

The EBSD mapping was conducted using a step size of 0.1 μm, implying that 1 pixel in the EBSD maps corresponds to 0.1 μm. The sampling radius for calculating the *AII* determines the length scale of the rough features to be characterized, and the calculation is using pixel as unit in the digital image. So the correlation between the physical length in μm and the length in the digital image measured by pixels should be clarified. The rough features with a small length scale on the boundary require small sampling radius. But if the sampling radius is smaller than 20 pixels, the error from pixelization of drawing the circles would be significant. To reduce this error, the original images have been enlarged by a factor of two using the MATLAB image processing toolbox, i.e.1 pixel in the new images corresponds to the physical length of 0.05 μm. The features on the boundary are preserved during this image-resize processing. As mentioned above, sampling radius no smaller than 20 pixels is then used to calculate *AII* with the new images. The boundaries used for calculation of *AII* are 1 pixel wide and pixels on the boundaries are connected with 4-neighbor connectivity.

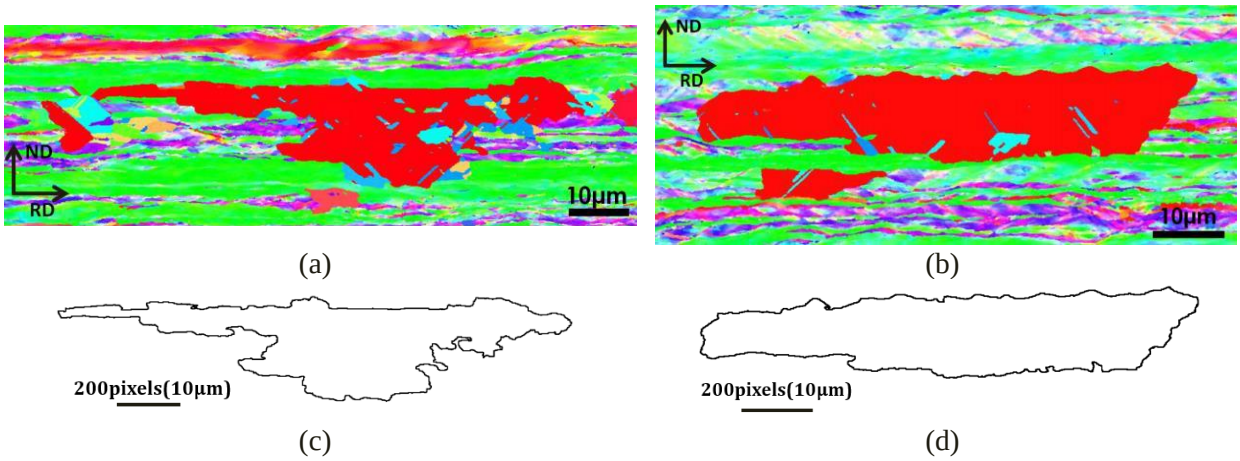

Figure 2. Electron backscattered diffraction (EBSD) images of CuSC1 (a) and CuSC2 (b). The boundaries surrounding the two grains are shown in (c) and (d). Interior twin boundaries are ignored during grain detection. Note that the boundaries showing in (c) and (d) are after pixel doubling of the original boundaries determined from EBSD maps.

The *AII* was calculated for both CuSC1 and CuSC2 at each pixel position along the boundaries using multiple sampling radii. In the following text, most results are obtained with a sampling radius of 40 pixels, corresponding to a physical length of 2 μm.

4. Results and discussion

Histograms of *AII* calculated for both CuSC1 and CuSC2 using sampling radius of 40 pixels (2 μm) are shown in figure 3. Both distributions show a clear peak at 0.5, which means that a major fraction of the two boundaries are relatively smooth at this length scale. The protrusions are revealed as the left tail of the distribution and the retrusions as the right. It is clear that the tails of the distribution are longer and bigger on both sides for CuSC1 than for CuSC2, which indicates that the rough features for CuSC1 are more prevalent than for CuSC2. Both distributions are not symmetric, and have longer tails on the retrusion side.

Larger retrusions than protrusions on a boundary have been observed from both experimental data and simulation [4, 6, 11]. The simulation has shown that in such a case the overall boundary migration rate can be affected [6]. Therefore the present asymmetry in the *AII* distribution shall be analyzed in more detail, for one protrusion and one retrusion with exactly the same morphology, $AII_r = 1 - AII_p$. Thus the distribution of $1 - AII_p$ could be directly compared with the distribution of AII_r.

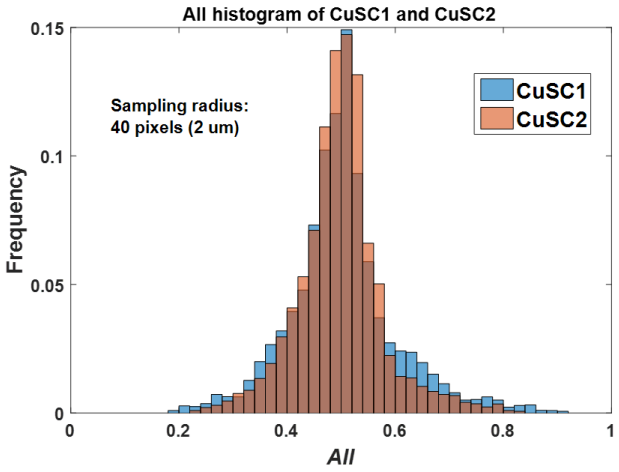

Figure 3. Histogram of *AII* for CuSC1 and CuSC2 calculated with a sampling radius of 40 pixels corresponding to 2 μm.

This comparison for CuSC1 and CuSC2 is shown in figure 4. For both boundaries, the tails of AII_r distribution are longer than those of $(1 - AII_p)$, implying that retrusions are sharper than protrusions and there are more sharp-retrusions than protrusions on both boundaries. More values of $(1 - AII_p)$ closer to 0.5 on both boundaries indicate that at the applied sampling scale the protrusions are "smoother" than retrusions. Figure 2(a) and (b) reveal sharp retrusions at the right bottom region of CuSC1 and at the bottom part of the boundary for CuSC2. By comparing figure 4(a) and (b), the tails for both $(1 - AII_p)$ and AII_r are longer for CuSC1 than for CuSC2, showing that both protrusions and retrusions are sharper on the boundary of CuSC1 than CuSC2 at the applied sampling scale, which corresponds with the visual impression from figure 2.

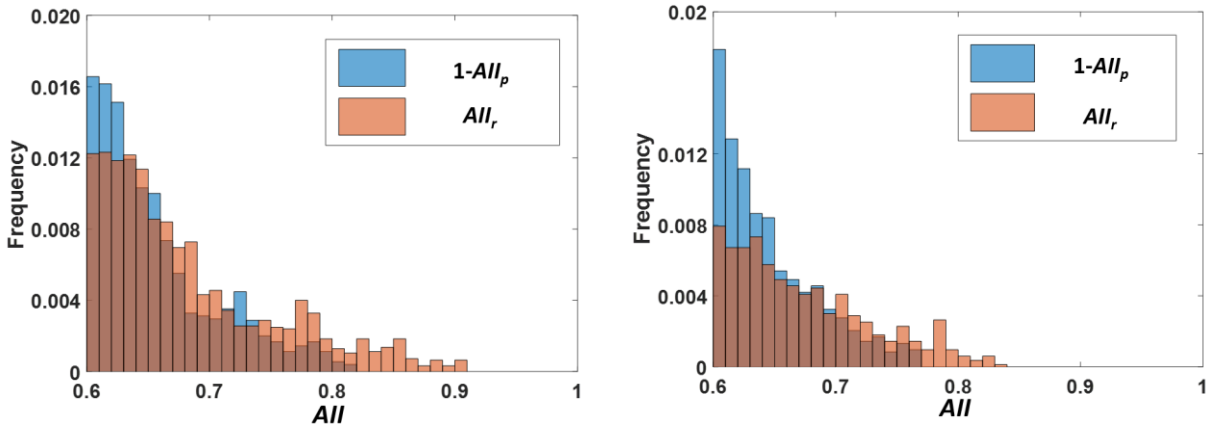

(a) (b)

Figure 4. Comparison between protrusions and retrusions for (a) CuSC1 and (b) CuSC2

The roughness parameters calculated based on the *AII* values shown in figure 3 for CuSC1 and CuSC2 are listed in table 2. The roughness parameters allow a direct quantitative comparison between the two boundaries from various perspectives. For all the roughness parameters listed, CuSC1 has larger values than CuSC2, which implies that on all aspects considered here, on the sampling scale of 40 pixels (2 μm), boundary CuSC1 is rougher than CuSC2. Also for both CuSC1 and CuSC2, the R_p values are smaller than R_r, consistent with the analysis above.

Table 2. Roughness parameters of CuSC1 and CuSC2 (sampling radius: 40 pixels corresponding to 2 μm)

Parameter	R_a	R_f	R_p	R_r	*Range*
CuSC1	0.198	0.255	0.329	0.390	0.721
CuSC2	0.157	0.165	0.303	0.363	0.602

To investigate if the roughness of CuSC1 and CuSC2 also differs on other length scales, roughness parameters are calculated with a sampling radius from 20 pixels (1 μm) to 250 pixels (12.5 μm). The results are shown in figure 5. It can be seen from figure 5(a) that at each length scale investigated, the boundary roughness R_a of CuSC1 is larger than that of CuSC2 and the difference increases at a larger length scale. With the increasing sampling radius, the boundary roughness of CuSC1 increases continually. This is because protrusions/retrusions of larger sizes are revealed with a larger sampling radius. While for CuSC2, R_a reaches a local maximum at about 50 pixels (2.5 μm), which means the largest protrusions/retrusions are mostly around this length scale. Referring to the morphology of CuSC2 (figure 2(d)), the protrusions/retrusions observable on the top and bottom parts of the boundary are approximately around this scale. R_a of CuSC2 starts to increase again with sampling radius larger than 150 pixels (7.5 μm), as both ends of the elongated grains are then tracked as protrusions by the *AII* calculation.

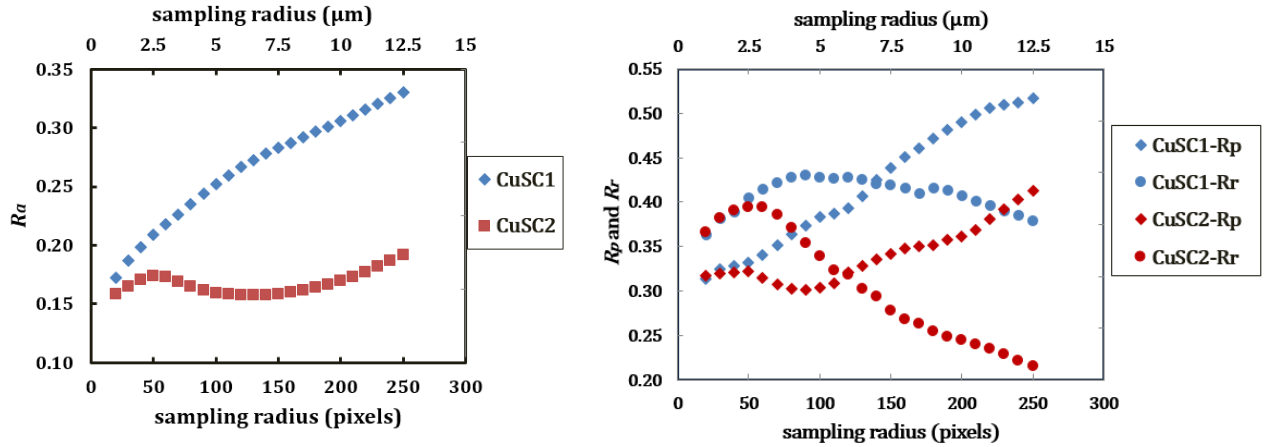

(a) (b)

Figure 5. Calculated roughness parameters for CuSC1 and CuSC2: (a) R_a and (b) R_p and R_r as a function of sampling radius.

The roughness variation considering only protrusions or retrusions is shown in figure 5(b). As discussed above at the sampling radius of 40 pixels (2 μm), the protrusions are "smoother" than retrusions. While with increasing sampling radius, the protrusions become the dominant rough features. As shown in figure 5(b), for CuSC1 R_p become larger than the R_r with a sampling radius above 140 pixels (7 μm), also for CuSC2,

R_p exceeds R_r with the sampling radius above 120 pixels (6 μm). The reason why R_p is higher for CuSC1 than CuSC2 at sampling radii above 50 pixels (2.5 μm) is that there are on CuSC1 several large branch-like features that have a scale larger than 2.5 μm on this boundary. It can also be observed that the retrusion roughness of CuSC2 (red circle) has a peak at a sampling radius of 60 pixels (3 μm), followed by a rapid decrease with increasing sampling radius, which leads to the observed local maximum in figure 5(a). While for CuSC1, the retrusion roughness is relatively steady, with a moderate peak at a sampling radius of 90 pixels (4.5 μm). The three calculated roughness parameters all demonstrate that CuSC1 is more irregular than CuSC2 at the length scales investigated. The visual difference of morphology and irregularity of the two grains as shown in figure 2 is clearly revealed from the roughness parameters. And this result corresponds well with the results obtained from previous work of boundary fractal analysis [15].

The EBSD images used for the current study were taken from the RD-ND plane for both specimens. Since in reality the recrystallizing boundaries are rough surfaces, one might wonder whether the characterization of protrusions/retrusions from a 2-dimensional image would represent the characteristics of real 3-dimensional structures. This of course cannot be verified for the present data, however, an 3-dimensional characterization of the recrystallizing boundaries in partly recrystallized aluminum has revealed the protrusions/retrusions appeared as ridges prolonged along TD [18], so the 2D microstructural characterization well indicates the rough features of the recrystallizing boundary.

5. Conclusions and outlook

A method is developed to quantitatively characterize the roughness of recrystallizing boundaries in partly recrystallized microstructures. Using the area integral invariant (*AII*) as a variable to obtain morphological information of the boundary, several parameters are calculated to quantify the boundary roughness. The potentials of these parameters in characterizing roughness are evaluated by comparing two copper grains with large visual differences in irregularity. It is found that:

(1) The visual impression of the grain CuSC1 being much more irregular than CuSC2 is quantified by the *AII* and the therefrom calculated roughness parameters;
(2) The roughness parameters are well suited to quantify possible differences in curvatures of the protrusions and retrusions. For the two grains investigated in the present work, it is statistically documented that larger curvatures exist at retrusions than at protrusions. This is important for the overall migration rate;
(3) By changing the sampling radii when measuring the *AII* it is possible to get information on the size distribution of both protrusions and retrusions.

Future efforts will be on further standardization of the method for boundary roughness quantification, and using this method to analyze the effects of protrusions/retrusions on boundary migration kinetics. Also the factors influencing the roughness of recrystallization boundary will be investigated.

Acknowledgement

The authors would like to thank the support from the Danish National Research Foundation (Grant NO.DNRF86-5) and the NSFC of China (Grant No. 51261130091) to the Danish-Chinese Center for Nanometals.

References

[1] Schmidt S, Nielsen S F, Gundlach C, Margulies L, Huang X X and Juul Jensen D 2004 *Science* **305** 229–32
[2] Van Boxel S, Schmidt S, Ludwig W, Zhang Y B, Juul Jensen D and Pantleon W 2014 *Mater. Trans.* **55** 128–36

[3] Zhang Y B, Juul Jensen D and Godfrey A 2012 *Mater. Sci. Forum* **715-716** 329–32
[4] Zhang Y B, Godfrey A and Juul Jensen D 2011 *Scripta Mater.* **64** 331–4
[5] Zhang Y B, Godfrey A and Juul Jensen D 2014 *Metall. Mater. Trans. A.* **45** 2899–905
[6] Moelans N, Godfrey A, Zhang Y B and Juul Jensen D 2013 *Phys. Rev. B.* **88** 1–10
[7] Juul Jensen D, Lin F X, Zhang Y B and Zhang Y H 2013 *Mater. Sci. Forum* **753** 37–41
[8] Martorano M, Sandim H, Fortes M and Padilha F 2007 *Scripta Mater.* **56** 903–6
[9] Drury, M R and Humphreys F J 1986 *Acta Metal.* **34** 2259–2271
[10] Martorano M, Fortes M and Padilha F 2006 *Acta Mater.* **54** 2769–76
[11] Zhang Y B, Godfrey A and Juul Jensen D 2009 *CMC* **3** 197-207
[12] Li J 2003 *Image-based Fractal Description of Microstructures*, Kluwer Academic Publisher
[13] Bérubé D and Jébrak M 1999 *Comput. Geosci.* **25** 1059–71
[14] Mandelbrot B, Passoja D and Paullay A 1984 *Nature* **308** 721–2
[15] Sun J, Zhang Y B, Dahl A B, Conradsen K and Juul Jensen D 2015 *IOP Conf. Ser.: Mater. Sci. Eng.* **82** 012006
[16] Manay S, Cremers D, Hong B W, Yezzi A J and Soatto S 2006 *IEEE.* **28** 1602–17
[17] Pottmann H, Wallner J, Huang Q X and Yang Y L 2009 *Comput. Aided Geom. Des.* **26** 37–60
[18] Zhang Y B and Juul Jensen D 2015 *Proc. 36th Risø Int. Symp. on Mater. Sci (Roskilde, DK, 2015)*, ed S Fæster et al (Roskilde: Risø).